

## The quantitative analysis of three action modes of volatile anesthetics on purple membrane

Tatsuo Nakagawa <sup>a,1</sup>, Toshiaki Hamanaka <sup>a,\*</sup>, Shinya Nishimura <sup>b</sup>, Ichiro Uchida <sup>c</sup>,  
Takashi Mashimo <sup>c</sup>, Yuji Kito <sup>d</sup>

<sup>a</sup> *Division of Biophysical Engineering, Department of Systems and Human Science, Graduate School of Engineering Science, Osaka University, Toyonaka 560-8531, Japan*

<sup>b</sup> *Intensive Care Unit, Osaka University Hospital, Suita, Osaka 565-0871, Japan*

<sup>c</sup> *Department of Anesthesiology, Osaka University Medical School, Suita, Osaka 565-0871, Japan*

<sup>d</sup> *TYK Laboratory for Photobiology, 55 Higashi-Minato, Yokata, Toyama 930-2243, Japan*

Received 27 December 1999; received in revised form 23 May 2000; accepted 26 May 2000

### Abstract

We quantitatively assessed the spectroscopic changes of purple membrane in relation to the concentrations of a volatile anesthetic. As reported previously, volatile anesthetics show three modes of action on purple membrane. By using an anesthetic for which the concentration in solution could be determined spectroscopically and by applying modified analytical methods regarding the M-intermediate lifetime, we were able to clarify the quantitative relation between anesthetic concentration and each mode of action, a relation which in the past has only been described qualitatively. We also determined through the measurement of transient pH changes with pyranine that the proton pump efficiency per photochemical cycle in an action mode induced with low concentrations of anesthetic does not change from that of the native state. Moreover, we dynamically obtained the individual M–bacteriorhodopsin difference spectrum of each state at room temperature using our flash photolysis system equipped with a wavelength-tunable dye laser. These results demonstrated again that we should clearly distinguish different action modes of anesthetics according to their concentrations. © 2000 Elsevier Science B.V. All rights reserved.

**Keywords:** Molecular mechanism of anesthesia; Bacteriorhodopsin; M-intermediate; Laser photolysis; Selective excitation; Transient pH measurement

### 1. Introduction

Anesthesia originates from the interaction between biomembranes and anesthetic molecules. Non-specific actions have been supposed because of the struc-

tural variety of anesthetic molecules (all lipophilic membrane perturbants including gases, hydrocarbons, halogenated hydrocarbons, ethers, halogenated ethers and other organic solvents can be anesthetics [1]) and/or the strong correlation between anesthetic potency and its solubility in lipids. Recently, however, it has been shown that several proteins change their activities at clinical concentrations of anesthetic, leading to a hypothesis attributing the specific actions of anesthetics to proteins [2]. Hot controversy

\* Corresponding author. Fax: +81-6-6850-6557.

<sup>1</sup> Present address: Unisoku Co., Ltd., Kasugano 2-4-3, Hirakata, Osaka 573-0131, Japan.

continues to surround these two contrary hypotheses.

We chose purple membrane (PM) as a good model biomembrane for the study of the molecular mechanism of anesthesia because it possesses the following favorable characteristics. PM is extracted purely from the cell membrane of halobacteria and contains a sole protein, bacteriorhodopsin (BR), and several types of lipids. The protein-to-lipid ratio is 3:1, which is a very high protein density [3]. Even in native PM, BR trimers form two-dimensional hexagonal lattices, resulting in the determination of three-dimensional structure of a membrane protein in atomic resolution [4]. BR is formed by seven hydrophobic  $\alpha$ -helices with intervening hydrophilic loops. In the center of BR, a retinal chromophore is covalently bound to Lys-216 via an  $\epsilon$ -Schiff base. The absorption of light triggers an isomerization of the chromophore from an all-*trans* configuration to 13-*cis*; BR is then transformed into several spectroscopically characterized intermediates, K, L, M, N and O, and then finally returns to its original state. This process is called the photochemical reaction cycle, and BR transports one proton from the cytoplasmic side to the extracellular side in a single cycle. The maximum wavelength of absorption ( $\lambda_{\max}$ ) of each intermediate depends on the electrostatic environments formed by amino acid residues around the  $\epsilon$ -Schiff base and whether the  $\epsilon$ -Schiff base is protonated or not. The  $\lambda_{\max}$  of the M-intermediates is at a much shorter wavelength than the other intermediates as its Schiff base is deprotonated, which means the M-intermediates are on the main stage of the proton pumping.

It is expected that the investigation of anesthetic actions on PM based on structural, functional and spectroscopic information as mentioned above may give us important suggestions to elucidate the mechanism of anesthesia at the atomic level. The interaction between PM and volatile anesthetics was first studied by Nishimura et al. [5] and was then investigated in detail by Uruga et al. [6]. There are three different modes of action on PM depending on the concentration of the volatile anesthetic. For low concentrations of anesthetic, the  $\lambda_{\max}$  shifts from the 569 nm of the native PM to 567 nm, the decay of the M-intermediate becomes fast, the efficiency of the proton pump is enhanced, and PM retains its crystallin-

ity. We name the BR in this state BR567 and this mode of anesthetic action mode I. Making use of the maintenance of this crystallinity, we showed by X-ray diffraction experiments that volatile anesthetic molecules bind to the protein–lipid interfacial region near the surface of the membrane [7]. For higher concentrations of anesthetic, the  $\lambda_{\max}$  shows a large blue shift to 480 nm, the M-intermediate lives longer, BR loses its proton pump function [6,8], and PM is no longer a crystal. We name this state BR480 and this mode of action mode II. Furthermore, several volatile anesthetics changed the  $\lambda_{\max}$  to 380 nm (similarly, BR380 and mode III) [5,9].

Other investigators who are studying interactions between anesthetics and PM, however, have hardly studied BR567/mode I because the difference between the native state and BR567 is small and the concentration range where mode I can be seen is narrow. As there is a possibility that mode I is related to clinical anesthesia, however, it is desirable to quantitatively determine the characteristics of mode I. If we could determine the dependence of the quantity of BR567 on the anesthetic concentration, the distinct characteristics of mode II is expected to be determined more clearly.

The purpose of this study was to determine the quantitative relation between different action modes of anesthetics and their concentrations. First, we observed the absorption spectrum changes of PM depending on the concentrations of four kinds of volatile anesthetics, and examined whether BR567, BR480 and BR380 were generated. We also tested whether anesthetized PM is denatured by light irradiation in order to determine its suitability in laser photolysis experiments. Next, to understand the photocycle of BR567 and BR480, we determined the spectra of the M-intermediates of BR567 and BR480 by performing polychromatic laser photolysis experiments for pure BR567 and BR480 as well as for a mixed sample of the two. Furthermore, we determined the accurate ratio of native BR/BR567/BR480 depending on the anesthetic concentration by using a volatile anesthetic whose concentration could be determined spectroscopically and by applying a modified analytical method to M-intermediate decay curves. We also used a pH indicator to test whether the enhancement of the proton pump efficiency in BR567 reported by Uruga et al. [6] is due to a real

enhancement of the efficiency per photocycle or to a shortening of the photocycle period. These experiments were made possible by our laser photolysis system equipped with a wavelength-tunable dye laser.

As a result, mode I is clearly distinguished from mode II and mode III, and different actions and sites of anesthetic molecules to biomembrane are strongly suggested dependent on anesthetic concentrations.

## 2. Materials and methods

### 2.1. Sample preparation

Native PMs were isolated and purified according to standard procedures [9]. The optical density (OD) of the PMs was approximately 20, and they were preserved at 4°C after the addition of 20 mM  $\text{NaN}_3$ . We adjusted the pH, salt concentration, and/or the concentration of the pH indicator, pyranine, just before each experiment.

### 2.2. Chemicals

The volatile anesthetics chloroform, methoxyflurane (1,1-difluoro-2,2-dichloroethyl methyl ether), and sevoflurane (fluoromethyl-1,1,1,3,3,3-hexafluoro-2-propyl ether) were obtained from Wako Pure Chemical Industries, Inc. (Osaka, Japan), Abbott Laboratories (trademark Penthrane; North Chicago, IL, USA) and Maruishi Chemicals (Osaka, Japan), respectively. These anesthetics are all well known clinically. The concentrations of the anesthetics were calculated by the amounts injected. We did not take into account the concentration decrease due to the partial evaporation of anesthetics during injections.

Trifluoroethyl iodide (TI) was obtained from Aldrich Chemical Co., Inc. (Milwaukee, WI, USA). Rudo and Krantz [10] have reported that TI results in stable anesthesia in monkeys; unfortunately, however, the anesthetic causes cardiac dysrhythmia in man. We can quantify the concentration of TI in solution by a spectrophotometer, for it has an absorption in the ultraviolet region ( $\lambda_{\text{max}} = 256 \text{ nm}$ ) where the absorption of BR is small. Its value is so large ( $\text{OD} > 5$ ), however, under the present experimental conditions that we actually used  $\text{OD}_{290}$ . The light scattering and the absorption of amino acid

residues with an aromatic ring, which might change in the process of BR480 production, also relate to  $\text{OD}_{290}$ . Their contributions to the absorbance change are, however, so small ( $< 0.03$  when  $\text{OD}_{569}$  of PM is  $\sim 0.1$ ) compared to the change of  $\text{OD}_{290}$  by the addition of TI ( $\sim 0.8$  at maximum concentrations) that the error of the concentration of TI is less than several percent.

The laser dye Stilbene 420, Coumarine 2 and Rhodamine 101 were purchased from Exiton, Inc. (Dayton, OH, USA). Pyranine (8-hydroxypyrene-1,3,6-trisulfonic acid, trisodium salt), a pH-sensitive dye, was purchased from Molecular probes, Inc. (Eugene, OR, USA).

### 2.3. Static absorption spectrum measurements

The absorption spectra of suspensions of native and anesthetized PM were measured by UV/Vis spectrophotometer V560 (Jasco, Tokyo, Japan) under thermal controls. We used Teflon- or glass-capped quartz cells with a path length of 10 mm.

### 2.4. Laser photolysis experiments

Laser photolysis experiments were performed using the improved time-resolved multichannel spectrophotometer system USP-500 (Unisoku Co., Ltd., Osaka, Japan). Fig. 1 shows the whole system. A two-way transparent quartz cell was set into a cell holder kept at the same temperature as the V560 spectrophotometer. The light source for the excitation of the sample was a YAG laser second/third harmonic or a compact tunable dye laser TSP-611 (Unisoku Co., Ltd.) pumped by the YAG laser Surelite I (Continuum, Santa Clara, CA, USA). The laser beams are polarized vertically and are set to be perpendicular to the monitor beam. For the monitor beam, a 150 W xenon lamp was used with its intensity properly reduced by an iris diaphragm. To avoid exposure of the sample to extra wavelength light, a color glass filter, and/or an interference filter were inserted between the monitor light source and the sample cell. After passing through the sample cell, the monitor light was split into two beams, with one directly entering the photomultiplier A and the other streaming into the spectrometer. The spectrometer had a path selection mirror at the exit, which

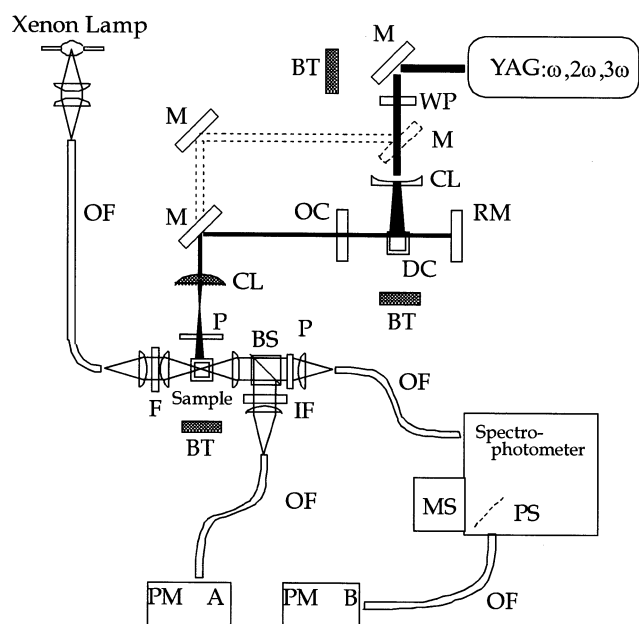


Fig. 1. Tunable dye laser equipped with a flash photolysis system. WP: 1/2 wave plate; BT: beam trap; CL: cylindrical lens; L: lens; RM: reflection mirror; DC: dye cell; OC: output coupler; M: mirror; OF: optical fiber; P: polarizer; F: filter; BS: beam splitter; IF: interference filter; PS: path selection mirror; MS: multichannel sensor; PM: photomultiplier.

could switch the direction of the light to photomultiplier B or a multichannel sensor (400 nm/512 ch). A notch filter was used behind the cell when using a YAG 532 nm light for excitations, and color glass filters were used if the second-order diffraction light of the grating was not negligible.

The maximum capabilities of this system are 10 ns and 1 ms sampling for monochromatic and polychromatic measurement, respectively. In the present monochromatic study, however, pseudo-log sampling acquisitions were performed from 100  $\mu$ s to 2 s after the excitation in order to record multiple components of lifetimes of different orders. The measurements were repeated, and the data were averaged. Reaction curves were fitted by one to four components of the exponential function by a non-linear least square analysis program (Unisoku), and the half-life ( $t_{1/2}$ ) and amplitude of each component were then obtained. In the polychromatic measurements, spectra from 300 nm to 700 nm were measured with 1 ms sampling. We also repeated the measurement and averaged data for every wavelength and every sampling time.

Before and after all laser photolysis experiments, we measured the static absorption spectrum to check that there was no denaturation.

### 2.5. Transient pH measurements

For the native PM and the PM containing pure BR567 obtained by saturated sevoflurane (see below), the transient pH changes induced by light absorption were obtained from the difference in the absorbance of pyranine between the buffered and the non-buffered sample [11]. The conditions were pH 7, 20°C and 150 mM KCl. As for buffered solution, 20 mM Tris was applied.

For both samples, the time courses of the absorbance changes were measured at 412 nm, the  $\lambda_{\max}$  of the M-intermediate, and at 455 nm, which is the  $\lambda_{\max}$  of pyranine and an isosbestic wavelength between the M-intermediate and the ground state. To correct for fluctuations in the excitation intensity, each data point was normalized by the peak height of the OD<sub>550</sub> change, which was simultaneously monitored by photomultiplier A.

## 3. Results

### 3.1. Absorption spectra of PM

Fig. 2 demonstrates the dependence of the spectral changes of PM on the concentrations of anesthetics. Differences in potency could be seen between different kinds of anesthetics. First, when chloroform was applied up to 5 mM, the spectrum changed slightly, and the  $\lambda_{\max}$  shifted to a shorter wavelength, that is, mode I was observed. Afterward up to 30 mM, the spectra changed drastically to the form of BR480, showing the action of mode II. When 50 mM chloroform was added, BR380/mode III was observed (Fig. 2a).

Methoxyflurane successively showed mode I and mode II actions with increasing concentration. At 20 mM, BR480 was produced almost perfectly (Fig. 2b). Even at a saturated concentration, methoxyflurane did not act on PM in mode III. As this BR480 was not denatured by intense illumination, it could be suitably used to observe the characteristics of pure BR480 in laser photolysis experiments.

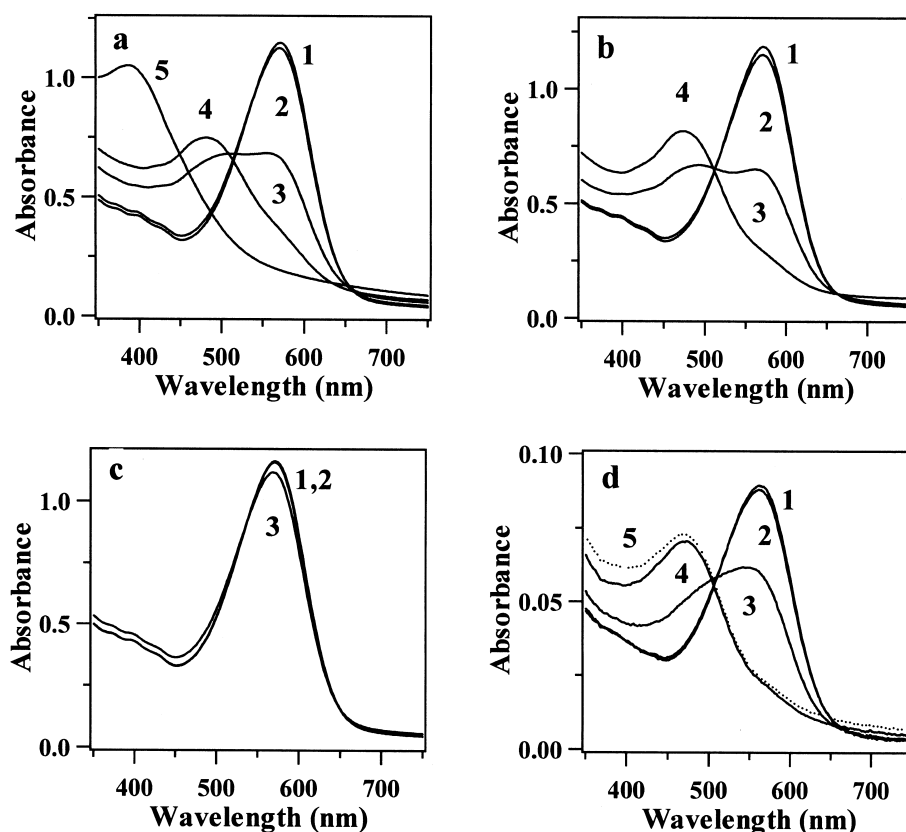


Fig. 2. The dependence of the absorption spectra of PM on the concentrations of four kinds of volatile anesthetics. 20°C, 20 mM phosphate, pH 6, 150 mM KCl. (a) Chloroform; curve 1: 0 mM; 2: 5 mM; 3: 15 mM; 4: 30 mM; 5: 40 mM. (b) Methoxyflurane; curve 1: 0 mM; 2: 2 mM; 3: 5 mM; 4: 20 mM. (c) Sevoflurane; curve 1: 0 mM; 2: 1 mM; 3: 10 mM. (d) TI; curve 1: 0 mM; 2: 5.6 mM; 3: 14 mM; 4: 32 mM; 5: 32 mM after exposure to room light. An irreversible generation of BR380 was observed. As for the sample containing TI, the OD of PM was one-tenth that of other samples in order to quantify the concentration of TI in the ultraviolet region where the absorption of PM is small.

As sevoflurane induced only BR567 even at saturated concentrations (Fig. 2c), it is considered to be appropriate for observation of the characteristics of pure BR567.

Like methoxyflurane, TI produced almost pure BR480, but an exposure to room light led irreversibly and gradually to the production of BR380 (Fig. 2d); therefore, a PM suspension containing high concentrations of TI (> 30 mM) does not appear to be appropriate for laser photolysis experiments. In Fig. 3, the absorbance changes at 590 nm and 450 nm are plotted against the concentrations of TI. The changes were small at 5 mM where mode I was dominant, and then large changes were induced by mode II. At concentrations over 15 mM, however, the changes slowed down, implying the process of BR567 to BR480 is not a simple single transition.

### 3.2. BR–M difference spectra of native PM

To determine the BR–M difference spectra, we performed a polychromatic time-resolved experiment using our multichannel system (Fig. 1).

To obtain a pure spectrum from each state of BR, it is desirable for none of the states to coexist with other states or to be denatured by repetitive excitations. As described above, pure BR567 is produced by saturated sevoflurane, and pure BR480 by saturated methoxyflurane, with none of these being denatured during the laser photolysis experiment. We then measured the transient spectral changes in these two samples and compared these spectra with that of the native BR. Curve 1 in Fig. 4 shows the difference between the spectrum after 2 ms and the one obtained before the excitation of native BR. The neg-

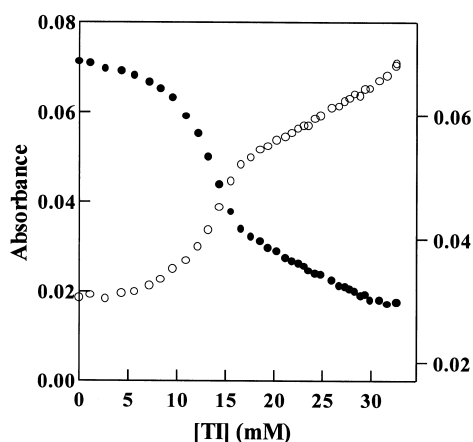


Fig. 3. The amounts of native BR and BR567 depending on the concentration of TI were monitored by the absorbance at 590 nm (filled circle) and that of BR480 was monitored at 450 nm (open circle). 20°C, pH 6, 150 mM KCl.

ative change in the longer wavelength region indicates the depletion of the ground state upon light excitation and the positive change in the shorter region shows the appearance of the M-intermediate. The maximum wavelength is 412 nm. We call this the native M (native BR) difference spectrum. Curve 2 is the difference spectrum for BR567 induced by the saturated sevoflurane. The positive peak also has its maximum at 412 nm, so we call this the M412 (BR567) difference spectrum. We could not detect a clear difference between M412 (BR567) and native M (native BR) except that there may be a slight shift of the negative peak wavelength to the shorter one. In the above two cases, the YAG laser second harmonic, 532 nm, was applied as the excitation light. Curve 3 shows the difference between the spectrum obtained 10 ms after the excitation and that of the ground state of BR480 obtained with saturated methoxyflurane. The longer wavelength region indicates BR480 depletion, whereas the shorter region indicates M-intermediate generation. The maximum wavelength is 365 nm, so we will call this M form M365 and call the spectrum the M365 (BR480) difference spectrum. In this case, a 446 nm dye laser pulse from Coumarine 2 was used for the excitation.

Next, we prepared a PM sample containing 5 mM methoxyflurane where BR567 and BR480 coexisted (see also Fig. 2b) and performed the same polychromatic experiment with different excitation wavelengths. When the sample was excited by the YAG

second harmonic, 532 nm, spectra with complex shapes and time courses were obtained (Fig. 5a, solid line). On the other hand, the excitation of the same sample by 621 nm light from the dye Rhodamine 101 induced almost the same spectrum as the M412 (BR567) difference spectrum (Fig. 5b, see also Fig. 4, curve 2) except for a small shoulder around 480 nm. In addition, the M-intermediate was quickly depleted (see curve 2 in Fig. 5b). This means that only BR567 could be excited selectively and M412 (BR567) has a short lifetime. In the same way, 424 nm light from the dye Stilbene 420 generated almost the same spectrum as M365 (BR480) difference spectrum (Fig. 5c, see also Fig. 4, curve 3) except for a minor shoulder around 570 nm. The M-intermediate was, moreover, slowly depleted (see Fig. 5c, curve 2). This strongly suggests that only BR480 could be excited selectively and M365 (BR480) has a long lifetime. Interestingly, the summation of spectra shown in Fig. 5b,c approximately produces the spectra shown in Fig. 5a (the summation is shown as a dotted line in Fig. 5a). This additivity means that the photocycle of BR567 and that of BR480 are independent of each other.

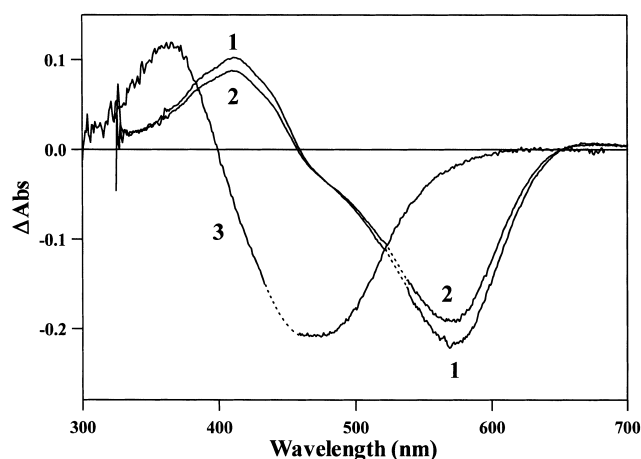


Fig. 4. The difference between spectra before and after the excitation. 20°C, pH 6, 150 mM KCl. Curve 1: native BR. The data before the excitation were subtracted from the data at 2 ms after the excitation. The excitation wavelength was 532 nm. Curve 2: BR567 (PM with saturated sevoflurane). The same conditions as for 1. Curve 3: BR480. The data before the excitation were subtracted from the data at 10 ms after the excitation with a 446 nm flash. Dotted lines in each profile are interpolated by hand because the flashlight was superimposed on the data at the excitation wavelength.

As for BR380, no spectrum changes were seen even when it was excited by the 355 nm YAG laser third harmonic (data not shown). These results indicate that the photochemical cycle is lost in BR380, which is consistent with the report by Mitaku et al. [8] that the retinal chromophore is free from protein in the state of BR380.

### 3.3. M-intermediate decay time

We performed high signal-to-noise (S/N) monochromatic laser photolysis experiments taking the following points into account. The use of too large an apparatus response time to smooth the noise or a too intense excitation/monitor light must be avoided

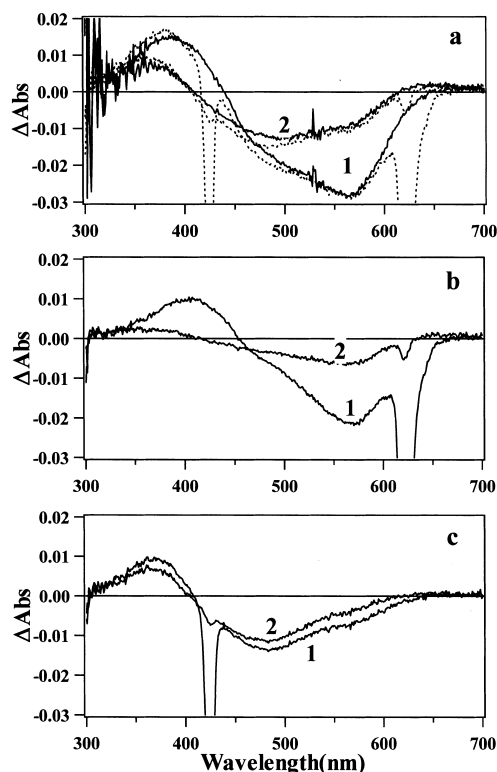


Fig. 5. The dependence of difference absorption spectra on the excitation wavelength. The sample was a PM suspension with 5 mM methoxyflurane where BR567 (by mode I) and BR480 (by mode II) coexist. Other conditions are 20°C, pH 6, 150 mM KCl. The excitation wavelengths were (a) 532 nm (solid line), (b) 621 nm, and (c) 424 nm. In each figure, the spectra designated 1 were obtained as the difference between the data at 1 ms after the excitation and the data obtained before the excitation. Spectra 2 show the differences between the data at 10 ms after and before the excitation. Broken lines in (a) are the summation of the spectra in (b) and (c).

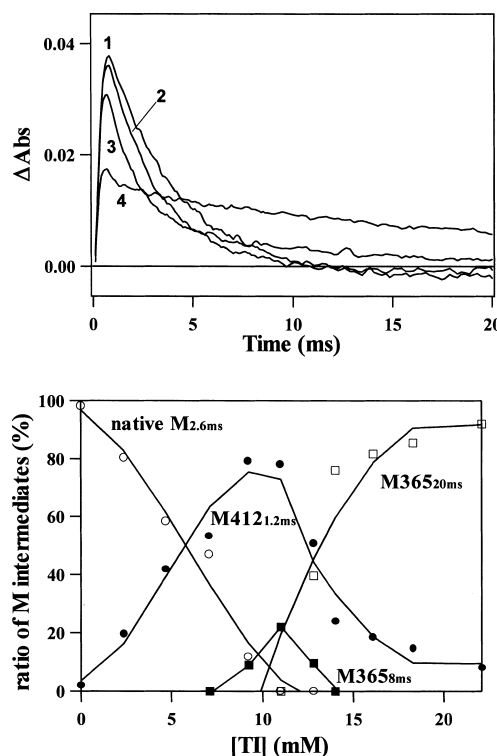


Fig. 6. (a) Transient absorbance changes of the M-intermediate obtained by monochromatic laser photolysis. 20°C, pH 6, 150 mM KCl. The excitation wavelength was 532 nm, and the observation wavelength was 375 nm. Curve 1: native PM; 2: PM with 4.6 mM TI; 3: 11 mM TI; 4: 22 mM TI. 20°C, pH 6. (b) The ratios of each M-intermediate to the whole of M-intermediates depend on the concentration of TI. These ratios are obtained from the amplitude of each component with a fixed lifetime calculated from the curves in (a). Also see the text. Open circle: native M for which the lifetime ( $t_{1/2}$ ) is 2.6 ms; filled circle: M412 from BR567 with a lifetime of 1.2 ms; filled and open square: M365s from BR480 with lifetimes of 8 ms and 20 ms, respectively.

because these conditions often induce artifacts. We therefore improved the S/N by reducing the optical losses and increasing the data accumulations. We set the excitation wavelength at 532 nm and the observation wavelength at 375 nm, points at which information regarding both M412 and M365 could be deduced. Additionally, an interference filter of 375 nm was put in front of the sample cell to avoid illumination by extra wavelength light. Because its precise concentration could be determined spectroscopically, TI was used as an anesthetic. Fig. 6a illustrates the selected decay curves.

We can see that the decay time of the M-intermediate gets faster at anesthetic concentration where

BR567 is generated (Fig. 6a, curve 2), while slow components appear at higher concentrations (Fig. 6a, curves 3,4), as reported for another volatile anesthetic [6,7].

At first, we treated both lifetime and amplitude as parameters in the fitting analysis, similar to the previous analyses. The results are shown in Table 1. At less than 9.2 mM, there is apparently a single component and its lifetime get shorter gradually as the anesthetic concentrations increase. At concentrations over 9.2 mM, a double-exponential function showed a good fit. We can see that shorter lifetimes are almost the same ( $\sim 1.2$  ms) in the concentration range from 9.2 to 18.3 mM. As shown in Fig. 5b, this component is attributed to M412 (BR567). Longer lifetime is  $\sim 7.5$  ms at 9.2 mM and 11.0 mM, then gets longer but comes to a constant value of 23 ms over 14.0 mM. Fig. 5c shows that this component is attributed to M365 (BR480). From the fact that almost constant values appeared for different anesthetic concentrations, we inferred that the M-intermediate in each state, native M, M412 (BR567) and M365 (BR480), has a fixed lifetime. As for the concentration of less than 9.2 mM, lifetimes vary from 2.60 ms to 1.75 ms, however, it is probable from the above finding that native M has a constant lifetime, 2.60 ms, and M412 (BR567) has a lifetime of approximately 1.20 ms, independent of the anesthetic concentration. Because 2.60 ms and 1.20 ms are too close to be distinguished in multi-exponential fitting analysis, the change in the ratio of native M/M412 (BR567) is considered to result in the observation of a single component with variable lifetimes.

Table 1

Calculated lifetimes and amplitudes (in parentheses) when both are treated as parameters in non-linear least square fitting analyses

[TI] (mM)	Lifetime 1 (ms)	Lifetime 2 (ms)
0	2.60 (100%)	–
2.4	2.30 (100%)	–
4.7	1.91 (100%)	–
7.1	1.75 (100%)	–
9.2	1.20 (83%)	7.17 (17%)
11.0	1.08 (78%)	7.68 (22%)
12.8	1.19 (75%)	15.9 (25%)
14.0	1.16 (55%)	23.3 (45%)
16.1	1.15 (46%)	24.1 (54%)
18.3	1.23 (39%)	22.9 (61%)

We therefore performed a revised fitting analysis in which the ratio of each state was treated as a parameter while the lifetime of each state was fixed regardless of the anesthetic concentration. From this analysis, we could deduce an accurate relation between the anesthetic concentration and the ratios of native BR/BR567/BR480.

If we assumed that there are four components, i.e.,  $t_{1/2} = 2.6$  ms for native M, 1.2 ms for M412 (BR567), 8 ms and 20 ms for M365 (BR480), respectively, we succeeded in achieving a good fit over the entire range of anesthetic concentrations only by altering the ratio of their amplitudes. The ratios were corrected for differences in absorbance at the excitation and observation wavelengths estimated from Figs. 2 and 4, respectively, and then plotted in Fig. 6b.

We previously reported a plot similar to Fig. 2b [12], but the more sophisticated present analysis gives us several new findings. The ratio of native M decreases slowly up to 10 mM, and M412 (BR567) increases instead. Though M412 (BR567) decreases drastically afterwards, it remains over 20 mM. M365 (BR480) appears as a component with an 8 ms lifetime at first, but another component with a 20 ms lifetime becomes dominant immediately. When we compare Fig. 6b with Fig. 3, the concentration region where the component with the 8 ms lifetime is seen (7–14 mM) corresponds to the region where dramatic amounts of BR480 are generated. On the other hand, the component with the 20 ms lifetime appears where the transition to BR480 slows down. If we plot the summation of the quantities of native M and M412 (BR567) versus the concentration of TI, it is well consistent with the curve of OD<sub>590</sub> in Fig. 3. Similarly, the plot of the summation of two components of M365 is well consistent with the curve of OD<sub>450</sub> in Fig. 3.

### 3.4. Transient pH changes and proton pump efficiency

As mentioned above, sevoflurane induced only BR567 by action of mode I even at saturated concentration (Fig. 2c). So we could get pure BR567 by saturated sevoflurane. In Fig. 7 the rises and decays of the M-intermediates (upper traces) and pH changes (lower traces) are shown for native BR in the absence of anesthetics (solid lines) and for BR567

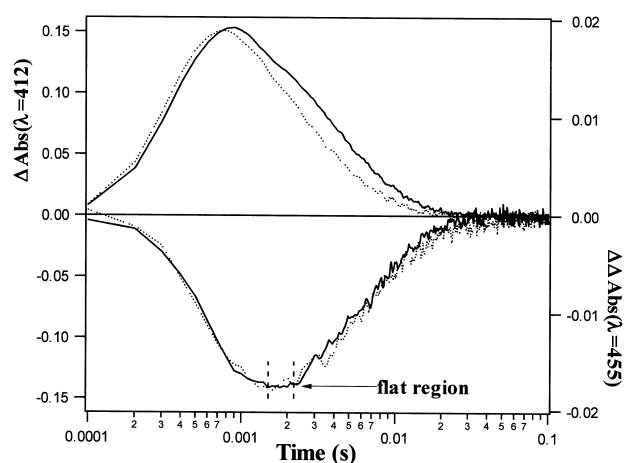


Fig. 7. Upper traces are the transient absorbance changes at  $\lambda=412$  nm, showing the rise and decay of the M-intermediate. Lower traces show the transient pH changes calculated from the absorbance difference at  $\lambda=455$  nm between the buffered and non-buffered samples containing the pH indicator pyranine. Solid line: native BR; dotted line: BR567 (PM with saturated sevoflurane). 20°C, 20 mM Tris, pH 7, 150 mM KCl. The horizontal axis is the logarithmic scale.

in the presence of saturated sevoflurane (dotted lines), respectively. The M-intermediate decay time for BR567, 2.2 ms, is smaller than that for native BR, 3.1 ms (these lifetimes are different from the above ones due to the difference in pH), while both decay times of pH changes are almost the same. There are flat regions in the pH curves, so the peak height of the pH transient curve normalized by the height of the M-intermediate absorbance curve gives the proton pump efficiency per photochemical cycle. We can see, from Fig. 7, the normalized height was almost the same in the cases of native BR (solid lines) and BR567 (dotted line).

Previously, Uruga et al. [6] prepared a vesicle containing BR oriented preferentially and measured the pH change under continuous illumination using a pH electrode; their results suggest that the proton pumping efficiency is enhanced in BR567. In the present experiment, the decay time of the M-intermediate of BR567 becomes faster than that of native BR, and also the recovery of OD<sub>550</sub>, which corresponds to the regeneration of the initial state, becomes faster from 4.0 ms to 3.1 ms (data not shown). This means that BR567 has a shortened photochemical cycle. Therefore, we conclude that the proton pump efficiency does not change in a single photochemical cycle

when BR is transformed to BR567 in response to anesthetic, but the period of the cycle is shortened.

#### 4. Discussion

Concerning the interaction between PM and anesthetic molecules, most investigators have paid more attention to BR480 (mode II) and BR380 (mode III), rarely even referring to BR567 (mode I) despite BR567 being clearly distinguishable from native BR and BR480 in terms of the proton pump efficiency (in the case of vesicles containing BR molecules), crystallinity, and lifetime of the M-intermediate [6]. In the present study, we confirmed three states of BR which are dependent on the concentration of anesthetics, and we also deduced the quantitative relation between the anesthetic concentration and the ratio of native M (native BR)/M412 (BR567)/M365 (BR480). The marked change in the ratio of M412 (BR567) versus anesthetic concentration shown in Fig. 6b is particularly noteworthy. Native M (native BR) no longer exists over 12 mM of TI, and M412 (BR567) is still present at rather high concentrations ( $\sim 20$  mM). Therefore, a sample with  $> 12$  mM of TI is a mixture of BR480 and BR567, not native BR. The selective excitation of BR567 by wavelengths longer than 600 nm where BR480 has little absorption is effective, if not perfect, in extracting information about the photocycle of BR567 (Fig. 5b). Similarly, information about the photocycle of BR480 can be effectively obtained from the selective excitation by wavelengths shorter than 450 nm (Fig. 5c). From Fig. 5, the M-intermediate with a short lifetime was identified as M412 (BR567) and the M-intermediate with a long lifetime was identified as M365 (BR480). Furthermore, it was proved that each photocycle is not affected by other photocycles from the correspondence between the spectra obtained by the simultaneous excitation of dual components (Fig. 5a, solid line) and the calculated spectra obtained by the summation of spectra measured by the selective excitation of single components (Fig. 5a, dotted line). Boucher et al. [13] have reported the BR–M difference spectra from a mixture of BR480 and BR567 by static low temperature spectroscopic methods using selective excitations through interference filters. Our data are consistent with theirs, and moreover, our

obtained spectra are much clearer than theirs in the points of the separation of different components and the transient property of each component, as the result of more effective excitation of BR480 or BR567 by a tunable dye laser and the dynamic measurements performed at room temperature.

In addition, the  $C_{50}$  value, the concentration giving a 50% response, can be obtained from Fig. 6b. The  $C_{50}$  value in mode I of TI for PM is estimated to be approximately 6 mM. By comparing with the spectra in Fig. 2, the  $C_{50}$  value for methoxyflurane and chloroform can also be estimated at  $\sim 2$  mM and  $\sim 5$  mM, respectively. On the other hand, the  $ED_{50}$  values, which are the concentrations that cause a loss of the righting reflex, are typically  $\sim 0.33$  mM for methoxyflurane and  $\sim 1$  mM for chloroform, several times smaller than the above  $C_{50}$  values. It has recently been reported that some proteins, for example GABA<sub>A</sub> receptor [14], alter their function at clinical concentrations of anesthetics, and they are considered to be candidates for targets of anesthetics by many investigators. We believe, however, that anesthesia is not caused by a change in a single specific protein function but is instead a result of amplification by multiple synaptic networks. Ueda and Kamaya [1] have discussed the effects of anesthetics on synaptic transmission reporting that a 10% inhibition of each synapse would result in a 65% reduction in the central neuronal system. Therefore, the  $C_{50}$  value for a single protein is considered to be meaningful when it does not deviate largely from the clinical concentration. Thus, we can consider the possibility that the same action as mode I in PM occurs generally in anesthesia.

We have previously reported that, in mode I, anesthetic molecules bind to the protein–lipid interface near the surface of PM based on X-ray diffraction experiments with heavy atoms containing the anesthetic molecule diiodomethane [7]. TI also contains a heavy iodine atom, and X-ray diffraction experiments show the same binding position as that found in diiodomethane [12]. As the environment near the surface of the membrane is hydrophilic, we think that the breaking of hydrogen bonds on the surface by anesthetic molecules slightly alters the state of BR. The capacity of anesthetics to break hydrogen bonds has been described theoretically by Sandorfy [15]. Recently, the relation between the proton pump

and the network of hydrogen bonds in the BR proton pathway has been explained in detail [16]. As Fig. 7 suggests, the proton pump efficiency per photochemical cycle does not change, but the velocity of the reaction increases; it is therefore considered that breaking hydrogen bonds on the surface affects the state of this hydrogen bond network, resulting in a slight rearrangement of amino acid residues near the Schiff base.

With regard to mode II, we could obtain interesting features of BR480 production in response to anesthetic concentration. In Figs. 3 and 6b, we can see that there is little production of BR480 or M365 at less than several mM of TI, thereafter it is produced drastically. We consider this sigmoidal characteristic is attributed not to cooperative binding of anesthetics to BR molecules but to the suppression of the BR480 production by the existence of BR567. As for this point and the fact that the transition from BR567 to BR480 is biphasic, however, details are future subjects.

In the present and previous studies, however, all of the volatile anesthetics [5–7,17,18] and local anesthetics [19] except for sevoflurane have been shown to induce BR480. Moreover, Uruga et al. [6] have shown that sevoflurane also induces BR480 in reconstituted PM in which the ratio of lipids to proteins is  $\sim 100$ . It is therefore thought that mode II may represent the general action of anesthetics. Uruga et al. [6] have shown by an X-ray diffraction experiment that PM containing BR480 loses its crystalline order, and Hamanaka et al. [12] have suggested based on a model calculation that anesthetic molecules enter into the internal domain of membranes. The changes in the potency of sevoflurane according to the protein/lipid ratio described above suggest that, in mode II, anesthetic molecules do not enter the protein interior but instead enter the hydrophobic lipid core. Therefore, the large change in  $\lambda_{\max}$  seen in BR480 is due to an allosteric change in the internal structure of BR through the action of anesthetics on the hydrophobic exterior region of proteins.

Finally, with regard to mode III, the suspension containing BR380 had the same  $\lambda_{\max}$  as the free *all-trans* retinal chromophore. This result is consistent with previously reported results [8] suggesting that the retinal chromophore loses the Schiff base bond with BR and that BR does not have a photochemical

cycle. The results of our diffraction experiment suggest that BR380 exists as a monomer (unpublished data). As this state is observed only when organic solvents or hydrocarbon-type volatile anesthetics are used, it is considered that the hydrophobic regions of anesthetic molecules enter deeply into proteins, greatly changing the conformation. This state is often irreversible, so we believe that it has no relation to the mechanism of anesthesia.

Different action modes of anesthetics according to their concentrations have been observed in other investigations. As for the protein-free membrane, it has been reported that anesthetic molecules first adsorb to the interface, then proceed into the lipid core, [20,21]. Mode I and mode II are considered to correspond to these two steps, respectively. The important difference is, however, that PM contains proteins. We think that the existence of proteins at high density in PM made mode I noticeable as shown in the present study. Although no crucial conclusion about the molecular mechanism of anesthesia can be obtained from the present data and their interpretation, the elucidation of the quantitative relation between anesthetic concentration and each mode offers fundamental information.

## References

- [1] I. Ueda, H. Kamaya, *Anesth. Analg.* 63 (1984) 925–945.
- [2] N.P. Franks, W.R. Lieb, *Nature* 310 (1984) 599–601.
- [3] D. Oesterhelt, W. Stoeckenius, *Nature New Biol.* 233 (1971) 149–152.
- [4] R. Henderson, J.M. Baldwin, T.A. Céska, F. Zelmin, E. Beckmann, K.H. Downing, *J. Mol. Biol.* 213 (1990) 899–929.
- [5] S. Nishimura, T. Mahimo, K. Hiraki, T. Hamanaka, Y. Kito, I. Yoshiya, *Biochim. Biophys. Acta* 818 (1985) 421–424.
- [6] T. Uruga, T. Hamanaka, Y. Kito, I. Uchida, S. Nishimura, T. Mashimo, *Biophys. Chem.* 41 (1991) 157–168.
- [7] T. Nakagawa, T. Hamanaka, S. Nishimura, T. Uruga, Y. Kito, *J. Mol. Biol.* 238 (1994) 297–301.
- [8] S. Mitaku, K. Ikuta, H. Itou, R. Kataoka, M. Naka, M. Yamada, M. Suwa, *Biophys. Chem.* 30 (1988) 69–79.
- [9] D. Oesterhelt, W. Stoeckenius, *Methods Enzymol.* 31 (1974) 667–687.
- [10] F.G. Rudo, J.C. Krantz Jr., *Br. J. Anaesth.* 46 (1974) 181–189.
- [11] Y. Cao, G. Váró, A.L. Klinger, D.M. Czajkowsky, M.S. Braiman, R. Needleman, J.K. Lanyi, *Biochemistry* 32 (1993) 1981–1990.
- [12] T. Hamanaka, T. Nakagawa, Y. Kito, S. Nishimura, I. Uchida, T. Mashimo, *Toxicol. Lett.* 100–101 (1998) 397–403.
- [13] F. Boucher, G.S. Taneva, S. Elouatik, M. Déry, S. Messaoudi, D.E. Harvey-Giran, N. Beaudoin, *Biophys. J.* 70 (1996) 948–961.
- [14] N.P. Franks, W.R. Lieb, *Nature* 367 (1994) 607–614.
- [15] C. Sandorfy, *Anesthesiology* 48 (1978) 357–359.
- [16] H. Lueche, H.-T. Richter, J.K. Lanyi, *Science* 280 (1998) 1934–1937.
- [17] S.G. Taneva, J.M.M. Caaveiro, I.B. Petkanchin, F.M. Goñi, *Biochim. Biophys. Acta* 1236 (1995) 331–337.
- [18] S. Messaoudi, K.-H. Lee, D. Beaulieu, J. Baribeau, F. Boucher, *Biochim. Biophys. Acta* 1140 (1992) 45–52.
- [19] L.S. Broun, B.K. Semin, I.I. Ivanov, A.A. Kononenko, S.K. Chamorovskii, A.A. Churin, *Biochemistry (USSR)* 56 (1991) 134–140.
- [20] S. Yokono, D.D. Shieh, I. Ueda, *Biochim. Biophys. Acta* 645 (1981) 237–242.
- [21] T. Yoshida, K. Takahashi, H. Kamaya, I. Ueda, *J. Colloid Interf. Sci.* 124 (1988) 177–185.